Non-equilibrium thermal behaviour of two main-chain thermotropic polymers

Evgeniy E. Pashkovsky*, Tamara G. Litvina, Anatolii I. Grigoriev, Anatolii Ya. Volkov, Andrej V. Tenkovtsev and Olga N. Piraner
Institute of Macromolecular Compounds, The Academy of Sciences, Bolshoi 31, St Petersburg 199004, Russia

(Received 31 January 1992; revised 6 November 1992)

The effect of thermal treatment on the thermodynamic properties and morphology of two nematic, thermotropic main-chain polymers with mesogenic groups containing 3,3′-biphenylene units and flexible spacers of different lengths has been studied by differential scanning calorimetry and X-ray scattering. An appreciable difference in the thermal behaviour of polymer samples with hexamethylene (BF6) and octamethylene (BF8) spacers was observed, despite identical thermal treatments. We found that BF6 samples had a crystalline structure after slow cooling from the isotropic state, whereas BF8 samples did not crystallize even at very slow cooling rates and possessed a glassy, nematic structure at room temperature. The enthalpy of the nematic–isotropic transition and the increase in the specific heat capacity at the glass transition for BF8 samples were greatly influenced by the rate used to cool the isotropic melt. This result is tentatively explained in terms of an improvement of the nematic ordering during cooling.

(Keywords: polymer liquid crystal; nematic–isotropic transition; thermodynamic parameters; heating rate dependence; thermal treatment)

INTRODUCTION

The dependence of the thermodynamic properties upon the molecular structure, molecular weight and the end groups of liquid-crystalline, main-chain thermotropic polymers has been reported[1–4]. It has been postulated in these investigations that the thermal properties for the nematic to isotropic (N–I) transition were measured under equilibrium conditions.

However, equilibrium conditions are fulfilled only if a high mobility of the polymer molecules exists in the nematic phase. Perhaps the suggestion about thermodynamic equilibrium is reasonable if the N–I transition occurs at high temperature. However, for polymers with low clearing temperatures, non-equilibrium behaviour must be taken into account, because at low temperatures the viscosity of the nematic melt is rather high and the time characterizing the process of relaxation of the thermodynamic parameters may be comparable with the duration of the thermal experiment. In this case, the parameters measured for the N–I transition (enthalpy ΔH_{NI} and temperature T_{NI}) will have non-equilibrium values.

The most evident example of non-equilibrium behaviour at the N–I transition was demonstrated by Keller *et al.*[5] for a main-chain thermotropic polyester with α-methylstilbene mesogenic groups (PHMS). Strong exponential dependences of the temperature T_{NI} and the enthalpy ΔH_{NI} on the annealing time t_a in the nematic state at $T = 120°\mathrm{C}$ were observed

$$T_{\mathrm{NI}} \sim \Delta H_{\mathrm{NI}} \sim 1 - \exp(-t_a/\tau) \qquad (1)$$

where the relaxation time τ is about 4 h; t_a is also measured in hours. These dependences were explained in terms of a non-equilibrium nematic phase with frozen-in disorder. Hence the nematic phase for PHMS contains defects which strongly influence the thermodynamic properties.

The change in the defect density with annealing time was studied for poly(ethylene terephthalate-*co*-*p*-oxybenzoate) (X7G) by Hashimoto *et al.*[6]. They found a power law dependence for d, the square root of the average area per disclination line, upon the annealing time t_a (at 240°C)

$$d \sim t_a^{0.35} \qquad (2)$$

where t_a was measured in seconds. Therefore the density of disclinations (defects) per unit area decays with time as $t_a^{-0.7}$. The corresponding relaxation time estimated according to the data given by Hashimoto *et al.* is $\tau = 3$ s. Comparison of the empirical equations (1) and (2) shows that a more rapid relaxation of the defect density is observed for X7G. This drastic difference in relaxation times for PHMS and X7G is undoubtedly caused by the difference in the annealing temperatures and the ranges of thermal stability of the nematic phase for X7G (180–370°C) and PHMS (103–172°C). These examples show that the non-equilibrium behaviour of main-chain polymers at the N–I transition may occur mostly for polymers with low T_{NI}.

---

* To whom correspondence should be addressed

0032-3861/93/234898-06

Hence, non-equilibrium phase behaviour for nematic polymers is not universal (as for semi-crystalline polymers), and one can expect the occurrence of different variants of thermodynamic behaviour of nematic polymers depending on chemical structure. We observed an example of unusual thermal behaviour in a main-chain polyester (with $T_{NI} = 130°C$) based on fumaroyl bis(4-oxybenzoylchloride) and trioxyethylene glycol[7]. We have found a strong dependence of certain thermodynamic parameters on the thermal history, caused by the existence of two different conformations of the monomer units in both the crystalline and nematic phases.

In this paper, we present the calorimetric study of the effect of thermal history on the thermodynamic parameters of the N–I transition for two semi-flexible polyesters containing 3,3′-biphenylene groups:

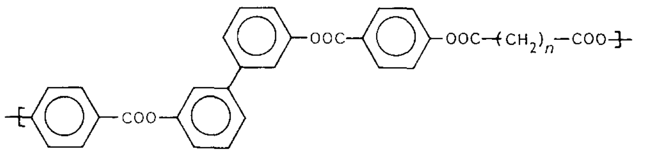

When $n = 6$, $\bar{M}_w = 52\,380$ (BF6) and when $n = 8$, $\bar{M}_w = 49\,920$ (BF8); $\bar{M}_w/\bar{M}_n = 2.0$ for both BF6 and BF8.

EXPERIMENTAL

The syntheses of polymers BF6 and BF8 are described in detail elsewhere[8]. The samples with maximum values of $\bar{M}_w$ were used in order to exclude the possible influence of molecular weight on the thermodynamic parameters.

We used differential scanning calorimetry (d.s.c.) (DSM-3 'Bioinstrument', Academy of Science, Puschino, Russia) with the calorimeter connected to a computer (DVC-3). All measurements were made in a dry nitrogen flow. Fresh samples (5–9 mg) were prepared for each measurement. The integration of peaks and determination of transition temperatures were carried out automatically. The accuracies of enthalpy and temperature determinations for standard samples were ±3% and ±0.5°C respectively. An In standard was used to calibrate the transition enthalpies. Calibration of the transition temperatures was carried out with In, Sn and Zn thermal standards. Two samples of sapphire with different masses were used for the specific heat determinations.

Polarizing microscopy observations were made with a hot-stage Boetius microscope (VEB Analitik, former GDR).

X-ray studies of polymer samples were performed on a DRON-3 (Russia) with direct recording of diffractograms. Ni-filtered CuKα radiation was used. All X-ray measurements were made at room temperature. The samples were prepared in the same calorimetric chamber as the samples for the d.s.c. study.

All samples were heated to $T > T_{NI}$ (200°C for BF6 and 150°C for BF8) and held for 15 min in the isotropic state. After that the samples were cooled at different rates (0.2–5 K min^{-1}) to room temperature. The heating thermograms were obtained in the temperature ranges 20–200°C for BF6 and 20–150°C for BF8 at a heating rate of 16 K min^{-1} in all cases.

RESULTS AND DISCUSSION

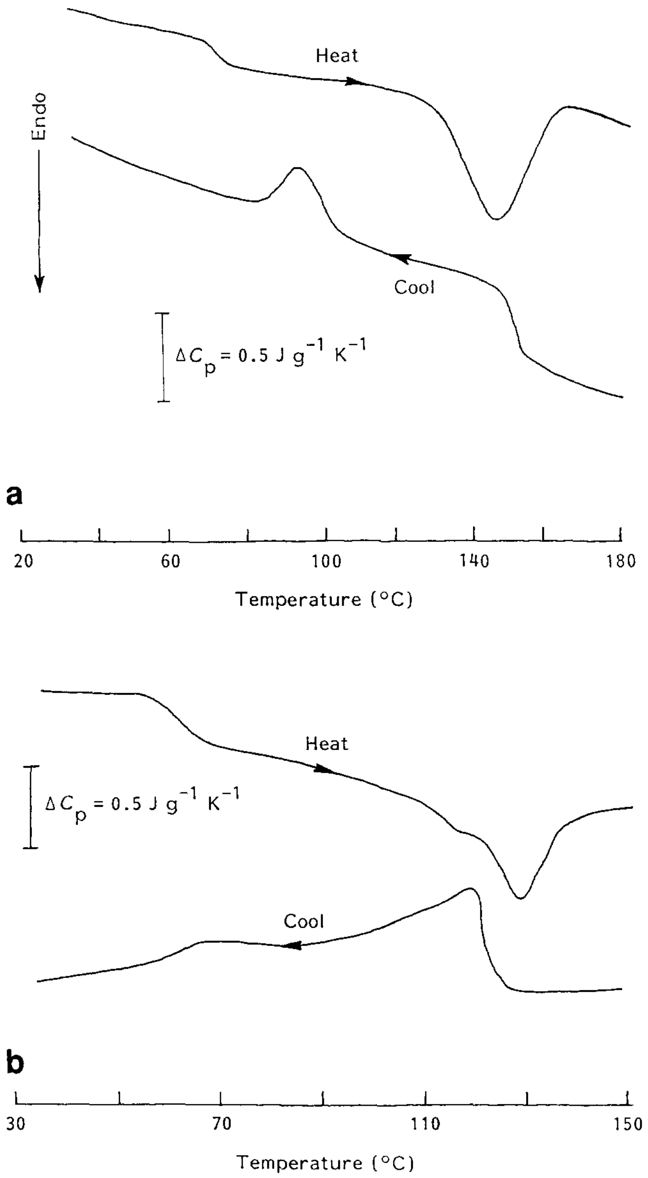

Figure 1 Thermograms for BF6 (a) and BF8 (b) obtained on heating as-synthesized samples and cooling from the isotropic melt with a scanning rate of 16 K min^{-1}

D.s.c. traces obtained on heating and cooling of the as-synthesized BF6 and BF8 samples are presented in *Figures 1a* and *1b* respectively. There are endothermic peaks corresponding to the N–I transition for both the polymers studied. The temperatures at which the samples were rendered isotropic, as observed with the polarizing microscope, corresponded to the onset temperatures of the endotherms in *Figure 1*. We did not observe any specific microscopic textures either of smectic or of nematic liquid crystals, probably because of the high molecular weights and viscosities of the polymer samples. The nematic structure of an anisotropic melt was evident from the wide-angle X-ray scattering data (see *Figure 2b*). The nematic glass–nematic melt transitions are clearly seen on thermograms for BF6 at 65–70°C and BF8 at 55–60°C (see *Figure 1*).

One can see from *Figure 1* the unusual behaviour of the BF6 and BF8 samples on cooling from the isotropic melt. There are no ordinary exothermic peaks corresponding to the I–N transitions for these samples. Instead of exotherms a decrease in the heat capacity C_p was observed at $T = 150°C$ for BF6 and $T = 120°C$ for BF8. These temperatures correspond to the clearing

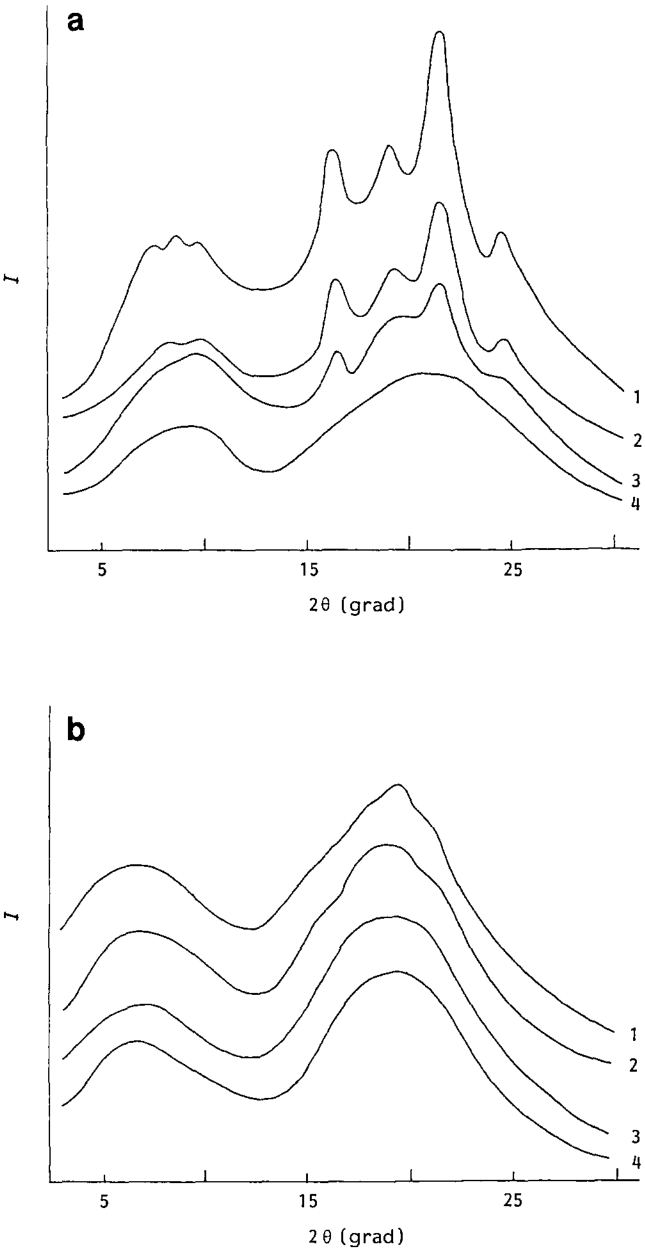

Figure 2 Diffractograms for BF6 (a) and BF8 (b) samples cooled from the isotropic melt at different cooling rates (Q in $\mathrm{K\,min^{-1}}$): (1) 0.3; (2) 1.0; (3) 3.0; (4) 130

points observed with the polarizing microscope. The values of ΔC_p corresponding to the I–N transitions are 0.386 and $0.408\,\mathrm{kJ\,mol^{-1}\,K^{-1}}$ for BF6 and BF8 respectively. These values of ΔC_p are somewhat larger than the values of ΔC_p for the glass transitions of the samples (see below, *Figure 6*). The low-temperature (97°C) exothermic peak on the cooling trace for BF6 can be ascribed to the crystallization process. The thermograms obtained on successive heatings are identical to those for the first heating run and are not shown in *Figure 1*.

The difference in character of the specific heat behaviour at the N–I phase transition on heating and on cooling can be explained by the differences in the thermodynamic properties and the structures of the nematic phases for samples on heating and on cooling. Therefore we studied the effect of thermal history (for example, cooling rate Q) on the thermodynamic properties and structures of the polymer samples.

Figure 2 gives two sets of diffractograms obtained at room temperature for BF6 (a) and BF8 (b), cooled from the isotropic melt with different cooling rates. The diffractogram for the rapidly cooled sample ($Q = 130\,\mathrm{K\,min^{-1}}$) consists of two 'amorphous' halos, centred at $2\theta = 8°$ and 22°. Diffractograms for samples of BF6 cooled with $Q < 3\,\mathrm{K\,min^{-1}}$ contain sharp maxima corresponding to the crystalline structure formed at low cooling rates. The intensities of these diffraction maxima increase strongly as Q decreases. Hence, for each sample under these conditions the degree of crystallinity α, estimated as the ratio of the area under the maximum to the total area under the diffractogram, is also increased.

Crystalline reflections in diffractograms for BF8 are absent (see *Figure 2b*). Only two halos centred at $2\theta = 8°$ and 18° were observed for these samples cooled with $Q = 0.2$–$130\,\mathrm{K\,min^{-1}}$. Hence, the samples of BF8 do not crystallize even at very low cooling rates. The difference in the ability to crystallize for the BF6 and BF8 samples can be ascribed to the different kinetic and thermodynamic parameters of crystallization for these polymers.

One can conclude from our data that two simultaneous processes, namely the melting of crystals and the rendering isotropic of the nematic phase, occur for BF6 samples previously cooled at $Q < 3\,\mathrm{K\,min^{-1}}$. The rendering isotropic of the BF8 samples includes only disordering of the nematic phase for all cooling rates used in this study.

Figure 3 gives the set of thermograms obtained on heating BF6 samples previously cooled with $Q = 0.2$–$3\,\mathrm{K\,min^{-1}}$. It is evident that the value of Q does not affect the appearance of the d.s.c. traces or the glass and phase transition temperatures. This trend is in contrast to the data obtained for BF8. The cooling rate strongly influences the area of the endotherm for BF8

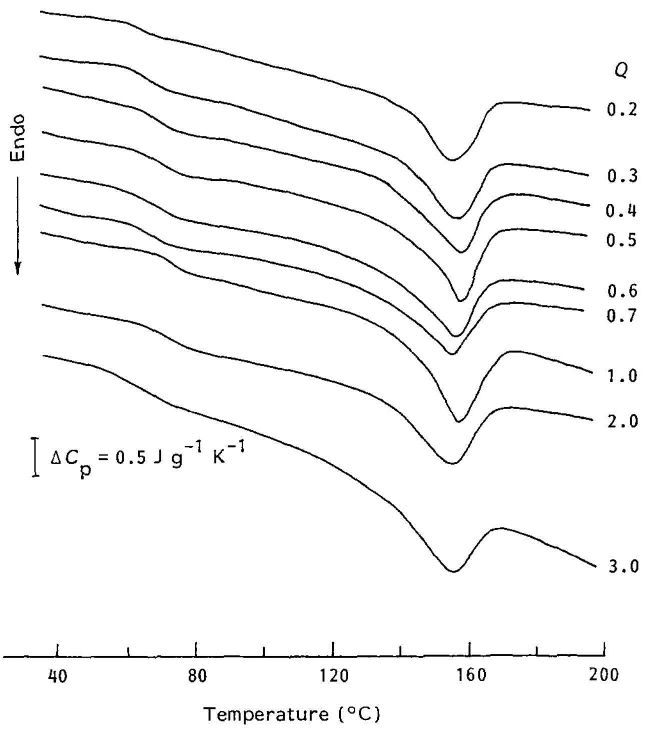

Figure 3 A set of thermograms obtained at a heating rate of $16\,\mathrm{K\,min^{-1}}$ for BF6 samples cooled from the isotropic melt at different cooling rates Q ($\mathrm{K\,min^{-1}}$). The values of Q are beside the curves

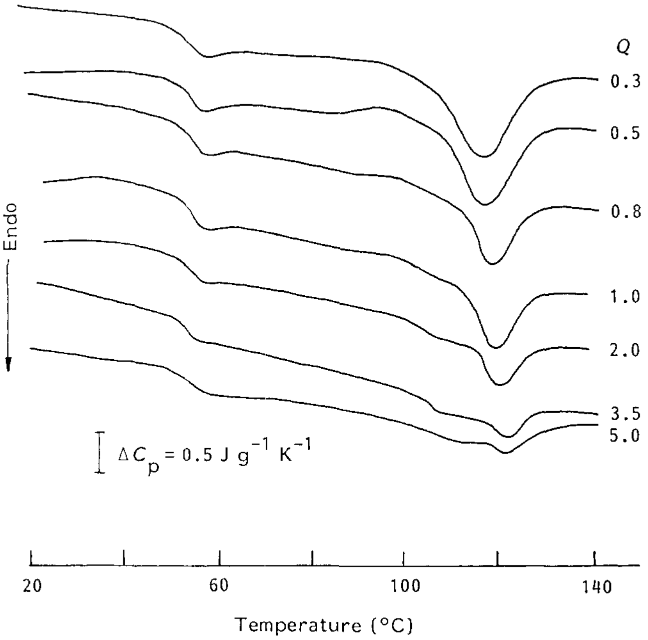

Figure 4 Thermograms for BF8 samples, obtained as described for *Figure 3*. The values of Q are beside the curves

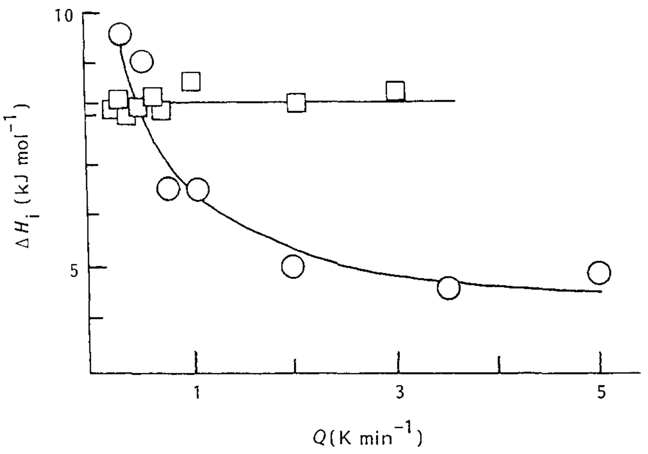

Figure 5 The dependence of the isotropization enthalpy $\Delta H_{\rm i}$ on the cooling rate Q for BF6 (□) and BF8 (○)

samples, as seen in *Figure 4*. The lower the value of Q, the larger is the peak area corresponding to the N–I transition for BF8. The dependence of the isotropization enthalpy $\Delta H_{\rm i}$ on cooling rate for BF6 and BF8 is presented in *Figure 5*. The value of $\Delta H_{\rm i}$ consists of two contributions for BF6 samples

$$\Delta H_{\rm i} = \Delta H_{\rm m}\alpha + \Delta H_{\rm NI}(1-\alpha)$$

or

$$\Delta H_{\rm i} = \Delta H_{\rm NI} + (\Delta H_{\rm m} - \Delta H_{\rm NI})\alpha \tag{3}$$

where $\Delta H_{\rm m}\alpha$ and $\Delta H_{\rm NI}(1-\alpha)$ are contributions connected with the melting of crystals and the N–I transition respectively and α is the degree of crystallinity. The dependence of $\Delta H_{\rm i}$ on Q given in *Figure 5* is the straight line $\Delta H_{\rm i} = 8.179 + 0.08Q$ (kJ mol^{-1}). One can replace the values of Q in the latter equation by the values of α calculated from the diffractograms presented in *Figure 2* for samples cooled at different rates. These values are $\alpha = 0.086$, 0.195 and 0.299 for $Q = 3.0$, 1.0 and 0.1 K min^{-1} respectively. These data fitted to equation (3) give the following values for transition enthalpies: $\Delta H_{\rm NI} = 8.5 \mp 0.065$ kJ mol^{-1} and $\Delta H_{\rm m} - \Delta H_{\rm NI} = -1.1 \mp 0.3$ kJ mol^{-1}. Therefore the small negative value of the slope for the dependence of $\Delta H_{\rm i}$ on Q is explained by the small value of $\Delta H_{\rm m} - \Delta H_{\rm NI}$ for BF6. This result for main-chain, liquid-crystalline polymers may be caused by the high degree of orientational and conformational order of the polymeric nematic phase. A more detailed study of the crystalline structure and the thermodynamic properties of BF6 could provide more information about the isotropization mechanism, including both the melting and the N–I transition. However, our general aim was to study the N–I transition itself without the simultaneous melting of crystals. Such a transition occurs for BF8 and the effect of thermal treatment on the N–I transition was investigated thoroughly for this polymer.

The dependence of $\Delta H_{\rm i}$ on Q has a quite different character for BF8 than for BF6 (*Figure 5*). A strong exponential increase in $\Delta H_{\rm i}$ at $Q < 2$ K min^{-1} was observed for BF8. We fitted the experimental dependence given in *Figure 5* to the exponential function

$$\Delta H_{\rm NI} = \Delta H_{\rm NI}(0) + [\Delta H_{\rm NI}(Q_{\rm max}) - \Delta H_{\rm NI}(0)]\exp\left[\frac{1}{k}\left(\frac{1}{Q_{\rm max}} - \frac{1}{Q}\right)\right] \tag{4}$$

The fitting parameters are: $\Delta H_{\rm NI}(0) = 11.57 \mp 0.61$ kJ mol^{-1}, $\Delta H_{\rm NI}(Q_{\rm max}) = 4.4 \mp 0.22$ kJ mol^{-1} and $k = 2.26$ min K^{-1} (k is a constant characterizing the rate of improvement of the nematic phase). The value of $\Delta H_{\rm NI}(0)$, corresponding to the cooling rate $Q = 0$, may be considered as an equilibrium value of the N–I transition enthalpy for a defect-free nematic sample. It should be noted that the value of $\Delta H_{\rm NI}$ in equation (3) is non-equilibrium because the improvement of the nematic structure is hindered by the crystallization for BF6 samples. The improvement of the nematic phase is evident from the d.s.c. data for BF8 samples. This supports the idea that defects greatly affect the thermodynamic properties of the polymeric nematic phase and the N–I transition enthalpy. Such a conclusion was also drawn for poly[hexamethyleneterephthaloyl-bis(4-oxybenzoate)] (PHTOB)[9,10]. The equilibrium value $\Delta H_{\rm NI} = 14.5$ kJ mol^{-1} was calculated by the analysis of phase equilibria in copolymers containing mesogenic units of PHTOB and non-mesogenic flexible units. The equilibrium value is higher than that obtained by direct d.s.c. measurements (8.6 kJ mol^{-1}).

Figure 6 presents the dependence of the heat capacity change $\Delta C_{\rm p}$ (at the nematic glass transition) on the cooling rate for BF6 and BF8. The value of $\Delta C_{\rm p}$ increases slightly with Q for BF6, whereas a strong exponential increase in $\Delta C_{\rm p}$ with Q is observed for BF8. The dependence of $\Delta C_{\rm p}$ on Q for BF8 was fitted to the equation

$$\Delta C_{\rm p} = \Delta C_{\rm p}(\infty) + [\Delta C_{\rm p}(0) - \Delta C_{\rm p}(\infty)]\exp(-Q/k') \tag{5}$$

The fitting parameters are: $\Delta C_{\rm p}(\infty) = 0.355 \pm 0.015$ kJ mol^{-1} K^{-1}, $\Delta C_{\rm p}(0) = 0.130 \pm 0.08$ kJ mol^{-1} K^{-1}, and $k' = 0.53$ K min^{-1} (0 and ∞ correspond to $Q = 0$ and $Q = \infty$). This result as well as the data for $\Delta H_{\rm NI}$ can be explained by the improvement of the nematic structure and the development of additional ordering for BF8 during slow cooling. The greater is this improvement, the smaller is the contribution of defects to the total values

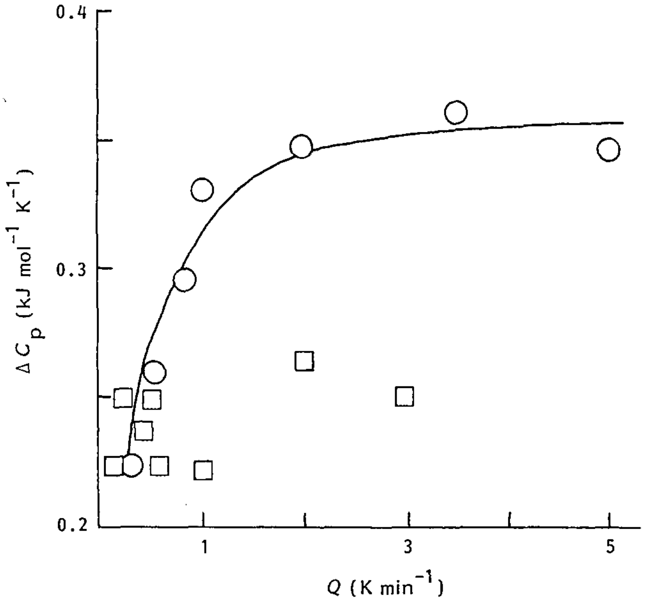

Figure 6 The dependence of the heat capacity change ΔC_p at the glass transition on the cooling rate Q for BF6 (□) and BF8 (○)

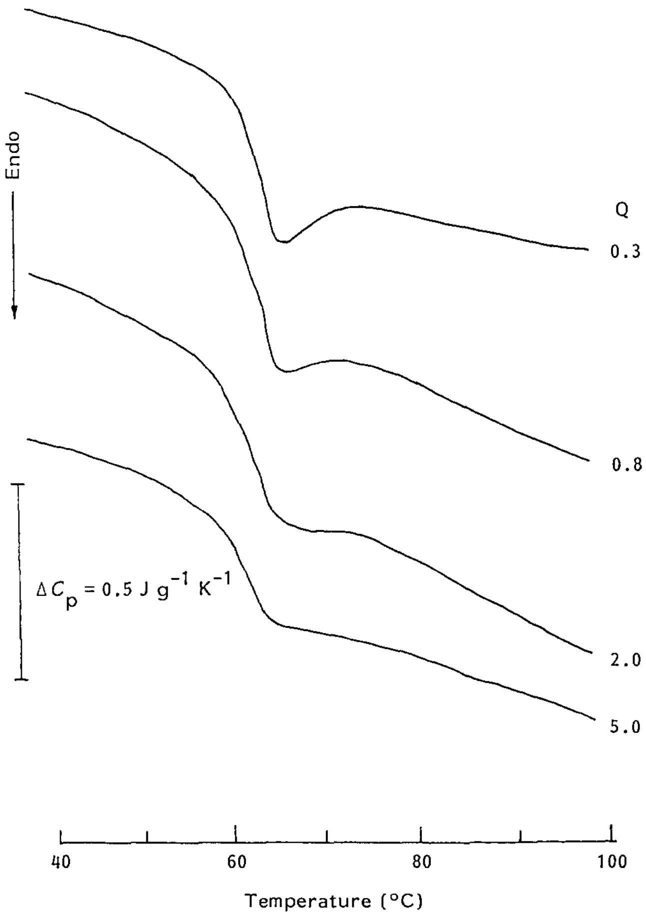

Figure 7 Fragments of thermograms in the region of the glass transition for BF8 samples cooled at different rates Q from the isotropic melt. The values of Q are beside the curves

of the enthalpy and specific heat of the nematic phase. Therefore the decrease in ΔC_p for slowly cooled samples is consistent with the data for the isotropic enthalpy (see *Figure 5*). One can estimate the value of the excess enthalpy of the nematic phase connected with such defects from

$$\Delta H_{\mathrm{def}} = \int_{T_1}^{T_2} [C_p^{\infty}(\mathrm{nem}) - C_p^{0}(\mathrm{nem})]\,\mathrm{d}T$$

$$= \int_{T_1}^{T_2} [\Delta C_p(\infty) - \Delta C_p(0)]\,\mathrm{d}T$$

$$= [\Delta C_p(\infty) - \Delta C_p(0)](T_2 - T_1)$$

where T_1 and T_2 are the temperature boundaries of the glass transition, and C_p^0(nem) and C_p^{∞}(nem) are the heat capacities of the nematic phase for samples cooled with $Q = 0$ and $Q = \infty$ respectively. The temperature interval of the glass transition $T_2 - T_1$ is about 30–35 K and ΔH_{def} is 6.6–7.7 kJ mol^{-1}. This value of ΔH_{def} is comparable with $\Delta H_{\mathrm{NI}}(0) - \Delta H_{\mathrm{NI}}(Q_{\mathrm{max}})$ which is 7.17 ∓ 0.82 kJ mol^{-1}.

It should be noted that for ordinary glasses and for amorphous polymers the enthalpy relaxation in the region of the glass transition causes a hysteresis effect[11,12]. This effect is connected with the relaxation of the free volume with temperature. For slowly cooled samples, this effect is endothermic because the number of holes increases with temperature. This effect cannot be seen from *Figure 4* because of the compressed scale, but it is evident from *Figure 7* which gives fragments of thermograms on an expanded scale for four samples cooled at different rates.

Endothermic effects for slowly cooled nematic glass samples are also observed. However, for amorphous polymeric glasses the cooling rate does not affect the value of ΔC_p, whereas for BF8 samples ΔC_p depends on Q. It is known that for semi-crystalline polymers the rise in the specific heat at the glass transition also depends on the thermal treatment because of the change in the degree of crystallinity α. The value of ΔC_p is a linear function of the amorphous phase content $(1-\alpha)$ of the semi-crystalline sample[13].

Nevertheless, the difference between nematic and crystalline polymers must be emphasized. The dependence of ΔC_p on the thermal history for semi-crystalline polymers is explained by the diminution of the amorphous phase content during thermal treatment. For nematic polymers, the content of the phase contributing to the glass transition is essentially independent of thermal history.

CONCLUSIONS

Thermal history was found to have a strong effect on the morphologies and the isotropization enthalpies of the two main-chain nematic polymers used in this study. For the polymer with the hexamethylene spacer (BF6), the isotropization includes two simultaneous processes: melting of crystals and isotropization of the nematic phase. The polymer with octamethylene spacers (BF8) does not crystallize and the only process that occurs is the isotropization of the nematic phase. A strong increase in ΔH_{i} for slow cooling rates Q is obtained. This result may be explained in terms of the improvement of the nematic structure of BF8 on slow cooling. The non-equilibrium phenomenon at the N–I transition for BF8 may be connected with the process of relaxation of the number of nematic defects which is observed experimentally as a relaxation of ΔH_{NI}. However, it is necessary to carry out more detailed structural investigations concerning the connection between thermodynamic properties and defects in the nematic structure. For example, it would be interesting to elucidate the role of biphenylene groups capable of conformational isomerism (from an extended 3,5 position to a non-linear 3,3′ position).

The thermal treatment of BF8 samples also affects the glass transition. The equilibrium value of the heat capacity rise $\Delta C_p(0)$ at the nematic glass–nematic melt transition is somewhat smaller than the value of $\Delta C_p(\infty)$ corresponding to samples with a non-equilibrium structure. We have also obtained endotherms after the glass transition for slowly cooled nematic BF8 samples. This result is consistent with the data for ordinary glasses and amorphous polymers.

REFERENCES

1 Blumstein, A. *Polym. J.* 1985, **17**, 277

2 Pashkovsky, E. E. *Usp. Khim.* 1987, **56**, 844

3 Pashkovsky, E. E., Bilibin, A. Yu., Skorokhodov, S. S. and Frenkel, S. S. *Vysokomol. Soedin., Ser. B* 1987, **29**, 74

4 Bilibin, A. Yu., Tenkovtsev, A. V., Piraner, O. N., Pashkovsky, E. E. and Skorokhodov, S. S. *Makromol. Chem.* 1985, **186**, 1575

5 Feijoo, J. L., Ungar, G., Keller, A. and Percec, V. *Polymer* 1990, **31**, 2019

6 Shiwaku, T., Nakai, A., Hasegawa, H. and Hashimoto, T. *Polym. Commun.* 1987, **28**, 174

7 Pashkovsky, E. D., Grigoriev, A. I., Volkov, A. Ya., Matveeva, G. N., Zvev, V. V., Bilibin, A. Yu., Skorokhodov, S. S. and Frenkel, S. Ya. *Vysokomol. Soedin., Ser. A* 1989, **31**, 129

8 Bilibin, A. Yu., Tenkovtsev, A. V. and Piraner, O. N. *Makromol. Chem.* 1989, **190**, 3013

9 Pashkovsky, E. E., Bilibin, A. Yu., Skorokhodov, S. S. and Frenkel, S. S. *Vysokomol. Soedin., Ser. A* 1987, **29**, 2544

10 Bilibin, A. Yu., Pashkovsky, E. E., Tenkovtsev, A. V. and Skorokhodov, S. S. *Makromol. Chem., Rapid Commun.* 1985, **6**, 545

11 Wunderlich, B., Bodily, D. M. and Kaplan, M. H. *J. Appl. Phys.* 1964, **35**, 95

12 Cheng, S. Z. D., Heberer, D. P., Janimac, J. J., Lien, S. H.-S. and Harris, W. F. *Polymer* 1991, **32**, 2053

13 Wunderlich, B. 'Macromolecular Physics', Vol. 1, Academic Press, New York and London, 1973, Ch. 4, equation (28)